Sensors and Actuators B 156 (2011) 779–783

Contents lists available at ScienceDirect

Sensors and Actuators B: Chemical

journal homepage: www.elsevier.com/locate/snb

Dispersive SnO_2 nanosheets: Hydrothermal synthesis and gas-sensing properties

Peng Sun, Yang Cao, Jun Liu, Yanfeng Sun*, Jian Ma, Geyu Lu*

State Key Laboratory on Integrated Optoelectronics, College of Electronic Science and Engineering, Jilin University, Changchun 130012, China

ARTICLE INFO

Article history:
Received 18 October 2010
Received in revised form 10 January 2011
Accepted 20 February 2011
Available online 25 February 2011

Keywords:
Tin oxide
Hydrothermal method
Nanosheet
Gas sensor

ABSTRACT

SnO_2 nanosheets with the thickness of 10 nm were successfully synthesized by a simple hydrothermal process at 180 °C for 12 h. The samples were characterized by X-ray power diffraction, scanning electron microscopy, transmission electron microscopy, and high-resolution transmission electron microscopy. The sensor performance of the as-prepared SnO_2 nanosheets for ethanol and carbon monoxide was measured. The results indicate that the sensor exhibited high response, quick response–recovery kinetics, and good repeatability.

1. Introduction

In recent years, great attention has been focused on synthesis and applications of one dimensional nanostructures materials such as nanowires, nanorods, nanobelts, and nanotubes [1–4]. Because of their unique structures and different specific properties from bulk materials, they have wide-ranging potential applications. On the other hand, two dimensional nanostructures are less thoroughly investigated. The properties and applications of two dimensional nanostructures are yet to be exploited. Metal oxides are the basis of smart and functional materials that have tunable properties and important technological applications. Among them, tin oxide (SnO_2), which has a large band gap (E_g = 3.6 eV at 300 K), is an important n-type semiconductor that has outstanding properties enabling its application in various fields, such as gas sensors [5–8], solar cells [9], and transistors [10]. Its properties highly depend on the synthesis method, size, morphology, crystal structure, and surface properties of the sample. Over the past years, several different morphologies of nanoscale SnO_2 have been synthesized via various methods [11–15]. However, until now, little attention has been given to the synthesis of dispersive SnO_2 nanosheets and exploration of their sensing properties.

Solution-phase synthetic strategy has attracted most attention in attempt to obtain metal oxides with different morphologies, due to its facile method, mild fabrication condition, and low cost. In this paper, we report the synthesis of dispersive SnO_2 nanosheets via a sodium citrate assisted hydrothermal process. The gas sensing properties of the sensors based on these dispersive SnO_2 nanosheets are examined.

2. Experimental

All the reagents were of analytical grade (Beijing Chemicals Co., Ltd.) and used as-received without further purification. In a typical procedure, $SnCl_2{\cdot}2H_2O$ (4 mM) and $Na_3C_6H_5O_7{\cdot}2H_2O$ (10 mM) were dissolved in a basic mixture of ethanol and water (1:1 by volume, pH ≈ 11) to form a homogeneous solution. The solution with dissolved precursor was magnetically stirred for 1 h before being transferred to a Telflon-lined stainless steel autoclave and then heated in an electric oven at 180 °C for 12 h. After the hydrothermal procedure, the autoclave cooled down to room temperature naturally. A yellow precipitate was collected after centrifugation and dried at 80 °C for 12 h. Finally, the sample was sintered at 400 °C for 2 h. The crystal structure and morphology of the obtained samples were characterized by X-ray power diffraction (XRD, Rigaku D/max-2500) with Cu Kα radiation (λ = 1.54056 Å), field emission scanning electron microscopy (FESEM, JEOL JSM-7500F, operated at 15 kV), transmission electron microscopy (TEM, JEOL JEM-200EX, operated at 200 kV), selected-area electron diffraction (SAED), and high-resolution transmission electron microscopy (HRTEM, JEOL JEM-3010, operated at 200 kV), respectively.

Gas sensors were fabricated as follows: the as-prepared powder was dispersed in the deionized water and ultrasonicated to make a paste, and then coated on an alumina tube (4 mm in length, 1.2 mm in external diameter, and 0.8 mm in internal diameter, attached with a pair of gold electrodes) by a small brush to form a thick film. The thickness of sensing films was about 100 μm. After drying under air at room temperature for 1 h, the devices were sin-

* Corresponding authors. Tel.: +86 431 85167808; fax: +86 431 85167808.
E-mail addresses: syf@jlu.edu.cn (Y. Sun), lugy@jlu.edu.cn (G. Lu).

0925-4005/$ – see front matter © 2011 Elsevier B.V. All rights reserved.
doi:10.1016/j.snb.2011.02.038

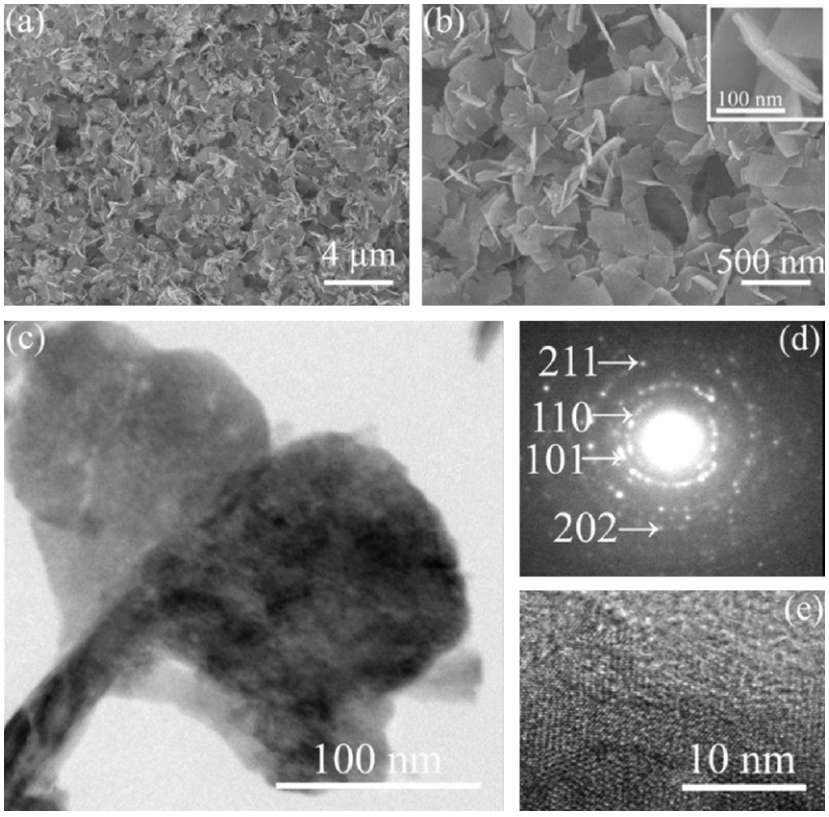

Fig. 1. Morphological characterization of as-synthesized SnO_2 samples: (a) panoramic, (b) enlarged FESEM images, (c–e) TEM, SAED, and HRTEM images of the nanosheets.

tered at 400 °C for 2 h. The operating temperature was controlled by adjusting the heating power, using a Ni–Cr alloy coil placed through the alumina tube. The sensing properties of the sensors were determined using a RQ-2 gas-sensing characterization system under laboratory conditions (50 RH %, 22 °C). The measurement was processed by a static process in a test chamber (50 L in volume). Environmental air was used as both a reference gas and a diluting gas to obtain desired concentrations of target gases. A typical testing procedure was as follows. The sensor was put into the chamber at the beginning. Then the calculated amount of the target gas or liquid was injected into the chamber by a microsyringe. When the response reached a constant value, the upper cover of the test chamber was removed and the sensor began to recover in air. For the target gases obtained from liquid, the concentration of target gas was calculated by the following formula,

$$C = \frac{22.4 \times \rho \times V_1}{M \times V_2} \times 100$$

where C (ppm) is the target gas concentration, ρ (g/mL) is the density of the liquid, V_1 (μL) is the volume of liquid, V_2 (L) is the volume of the chamber, and M (g/mol) is the molecular weight of the liquid. The gas response S was defined as the ratio Ra/Rg, where Ra and Rg are the resistances measured in air and the tested gas atmosphere. The response and recovery time were defined as the time taken by the sensor to achieve 90% of the total resistance change in the case of adsorption and desorption, respectively.

3. Results and discussion

The morphology, structure, and size of the SnO_2 nanosheets were characterized with FESEM, TEM, and HRTEM. Fig. 1a is a typical low-magnification scanning electron microscopy (SEM) image of the as-synthesized sample, from which a number of uniform nanosheets were clearly observed. No other morphologies could be detected, indicating a high yield of these nanosheets. The high-magnification SEM image of sample is shown in Fig. 1b. It can be seen that the nanosheets were mostly rectangular in shape, but some of them exhibited irregular shapes. Higher magnification SEM image of nanosheet is shown in the inset of Fig. 1b. As can be seen from it, the surface of the SnO_2 nanosheet was rather smooth, and the thickness of the SnO_2 nanosheet was about 10 nm. The typical TEM image in Fig. 1c shows that the size and shape of SnO_2 were similar to those of the FESEM observations. The corresponding SAED pattern (Fig. 1d) and the HRTEM image (Fig. 1e) confirm

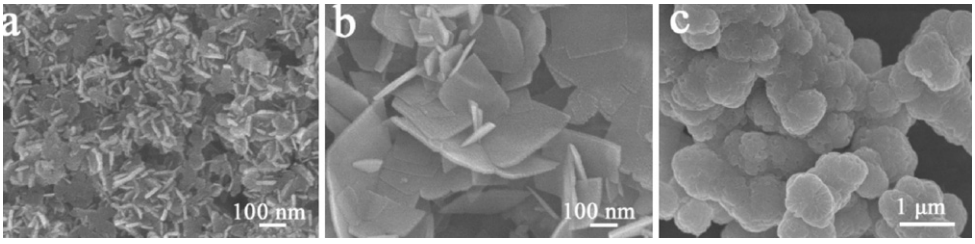

Fig. 2. FESEM images of samples obtained by using (a) 5 mmol sodium citrate, (b) 10 mmol sodium citrate, (c) 0.9 g PVP.

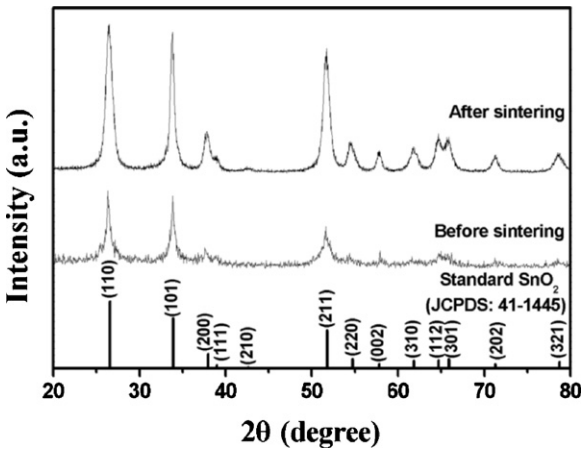

Fig. 3. XRD patterns of the as-prepared SnO_2 samples before and after sintering.

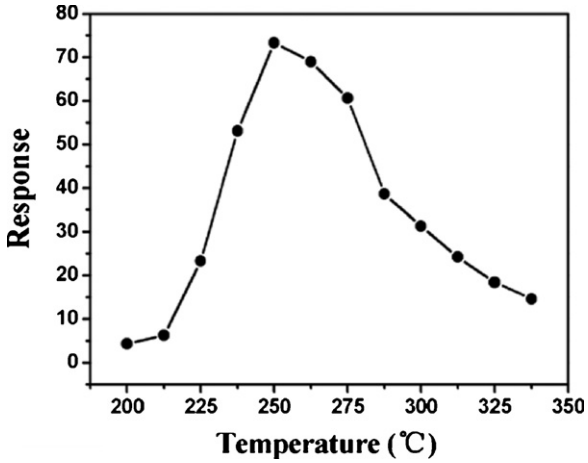

Fig. 4. Response of the sensor to 100 ppm ethanol as a function of operating temperature.

that the SnO_2 nanosheets were polycrystalline structures in nature.

To investigate the role of sodium citrate in the formation of SnO_2 nanosheets, the controlled experiments of the hydrothermal process with different concentrations of sodium citrate and with replaced poly (vinyl pyrrolidone) PVP had been carried out, respectively, keeping other experimental conditions constant. When the concentration of sodium citrate was 5 mM, it could be observed that the sample consisted of large number of smaller nanosheets (Fig. 2a). The increasing of the concentration (10 mM) led to the generation of relatively dispersive nanosheets (Fig. 2b). When we used PVP as a surfactant instead of sodium citrate, the as-synthesized sample consisted of a large scale of rugged microspheres with the sizes of 800 nm to 1 μm (Fig. 2c). On the basis of above results, it can be concluded that sodium citrate plays an important role in forming SnO_2 nanosheets.

The typical XRD patterns of the SnO_2 nanosheets before and after sintering are shown in Fig. 3. All the diffraction peaks from the sample could be very well indexed to tetragonal rutile structured SnO_2 with the lattice parameters of $a = 4.738$ Å and $c = 3.187$ Å, which was consistent with the standard data file (JCPDS file no. 41-1445). No other diffraction peaks were observed. After sintering, diffraction peaks in the XRD pattern suggested that the sample was of high crystallinity. Compared with those of the bulk material, the peaks were relatively broadened, which demonstrated that the SnO_2 had a small crystal size. The mean crystallite size was calculated to be around 11 nm using the Debye–Scherer formula, $D = 0.89\lambda/(\beta \cos\theta)$, where λ is the X-ray wavelength, θ is the Bragg diffraction angle and β is the peak width at half maximum. The calculated value almost accords with the thickness of nanosheet observed from the SEM image (inset of Fig. 1b).

The sensing properties of the sensor using uniform SnO_2 nanosheets were investigated. In order to determine the optimum operating temperature, the response of the SnO_2 nanosheets sensor to 100 ppm ethanol was tested as a function of operating temperature, as shown in Fig. 4. The response increased with a raise of operating temperature and reached the maximum value of 73.3 at 250 °C, followed by a decrease with further increase of operating temperature. Therefore, the optimal operating temperature of 250 °C was chosen for ethanol, to further examine the characteristics of the sensor.

Fig. 5a shows the gas responses of the SnO_2 nanosheets-based sensor to various testing gases of 100 ppm at the operating temperature of 250 °C. Eight kinds of volatile organic compound (VOC) gases were tested, including ethanol, butanone, acetone, etc. In Fig. 5a, the results indicate that the sensor using SnO_2 nanosheets exhibited lower responses to acetone, isopropanol, toluene, methanol, and butanone than that of the response to ethanol, and were almost insensitive to dimethylbenzene and formaldehyde. The highest response of the sensor was about 73.3 to ethanol, while the responses to other gases were no greater than 33. The different responses observed toward different carbon compounds can be ascribed to their polar character. Test gas molecule with strong polarity is more easily decomposed and oxidized than that with weak one [16].

The relationship between response and ethanol concentrations for the sensor at operating temperature of 250 °C is depicted in Fig. 5b. From the curve, it is found that the response increased with the increase of ethanol concentration from 20 to 1100 ppm. When the ethanol concentrations reached higher levels, the response almost tended to saturation. When the ethanol concentrations

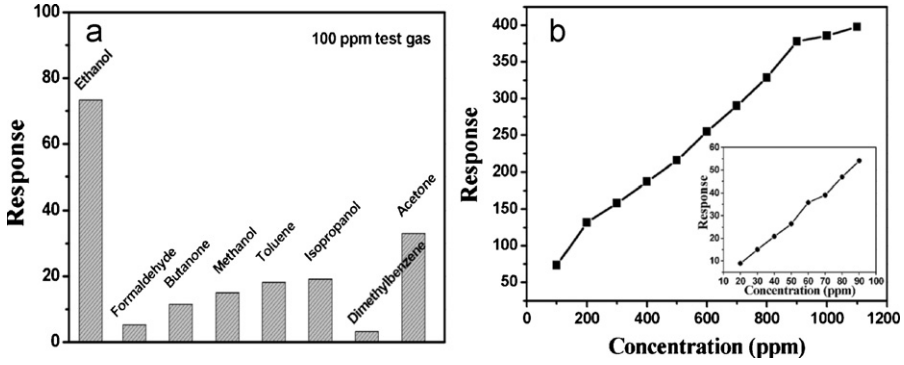

Fig. 5. (a) Responses of the sensor using SnO_2 nanosheets to 100 ppm various test gases at 250 °C. (b) Response of the sensor versus the ethanol concentration at 250 °C.

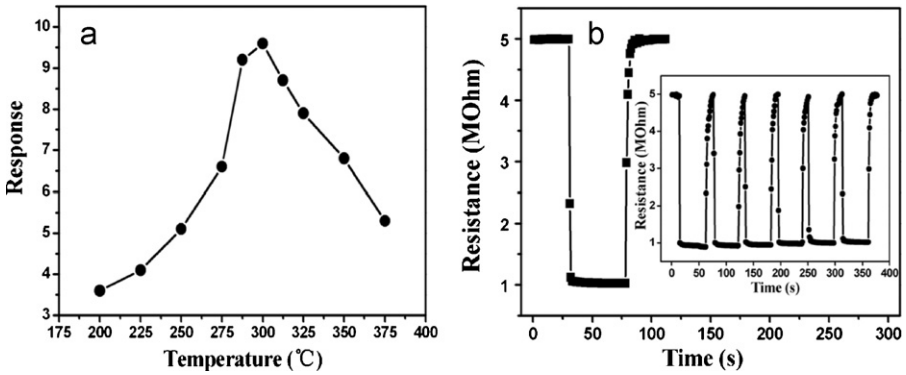

Fig. 6. (a) Response of the sensor using SnO_2 nanosheets to 500 ppm CO as a function of operating temperature. (b) Response transients of the sensor to 200 ppm CO at 300 °C, the inset displaying six periods of response curve.

were in the range of 20–90 ppm, it should be noted that the linear dependence of the responses on the ethanol concentrations is observed, as shown in the inset of Fig. 4b. Specifically, the sensor using SnO_2 nanosheets was found to exhibit high responses to ethanol gas even at low concentrations. Compared with the sensing properties of other SnO_2 nanostructure sensors [17–19], the advantage of our SnO_2 sensors is a relatively higher response to ethanol gas, so it can be expected to serve as a promising functional material in ethanol gas sensors.

For the gas sensing mechanism of SnO_2 nanosheet-based sensor, it should follow the surface charge model, which may be explained by the change in resistance of the sensor upon exposure to different gas atmospheres. When the sensor is exposed to air, oxygen molecules are adsorbed on the surfaces of the SnO_2 nanosheets and ionized to O_2^-, O^- or O^{2-} by capturing free electrons from the conductance of SnO_2 nanosheets, which results in the increase of resistance of the sensor. When the sensor is exposed to a reducing gas such as ethanol, these gas molecules can react with adsorbed oxygen species on the surface of SnO_2 nanosheet. This process releases the trapped electrons back to the conduction band and finally leads to a decrease in the resistances. In addition, the high response is attributed to the small size of the SnO_2 nanosheets. For n-type semiconductor metal oxides, if the size of them is reduced to a scale comparable to the space-charge layer thickness, the oxide should show high sensitivity to a target gas [20,21].

Gas-sensing properties of the sensor based on SnO_2 nanosheets to carbon monoxide were also investigated. Fig. 6a presents the relationship between the responses to 500 ppm CO and the operating temperature for the sensor based on SnO_2 nanosheets. It is clear that the operating temperature had an obvious influence on the response of sensor to CO. The responses of the sensor increased and reached maximum at 300 °C, and then decreased rapidly with further increasing the operating temperature. It is considered that 300 °C was the optimum operating temperature for the sensor using SnO_2 nanosheets. Therefore, the temperature of 300 °C was chosen for further examining the gas-sensing properties of the sensor to CO gas.

The response and recovery characteristics to 200 ppm CO at operating temperature of 300 °C were investigated, and the curve is shown in Fig. 6b. The results indicate that the SnO_2 nanosheet-based sensor had a fast response–recovery process. The response and recovery times of the SnO_2 nanosheet-based sensor were about 1 and 3 s, respectively. Compared with the sensing properties of sensors using other SnO_2 nanostructure [22–24], it could be seen that the SnO_2 nanosheet-based sensor had a relative shorter response and recovery times. Although, some sensors exhibit relatively higher response compared with our work, the potential applications, such as rapid and continuous detection, were limited due to the longer response and recovery times. Therefore, the advantage of our SnO_2 sensors is the relatively shorter response and recovery times. Six reversible cycles of the response curve indicated that the sensor had good repeatability and stability, as shown in the inset of Fig. 6b. The fast response and recovery times and good repeatability of the SnO_2 nanosheet-based gas sensor support its promising applications at the industrial level. The fast response and recovery times may be ascribed to the framework of gas diffusion toward the SnO_2 surface and its reaction with surface absorbed oxygen [25]. The response and recovery times of the sensor are influenced by several factors such as the gas diffusion, the thickness of sensing layer, and the amount of gas adsorption on the sensing material at different operating temperatures [26–28]. At a constant temperature, the amount of target gas and the surface reaction between the gas and the adsorbed oxygen will not vary significantly. Accordingly, the diffusion of oxygen and reducing gases toward the surface of the sensing material could be regarded as the key factor. Nano-sized particles are generally used to maximize the response [29]. However, significant aggregation between particles is inevitable due to the van der Waals attractions. Thus, for the target gas, it is difficult to diffuse through the nano-scale pores in the aggregates. In contrast, gas diffusion toward the surfaces of SnO_2 nanosheets is relatively easy due to many channels and pores between the SnO_2 nanosheets.

4. Conclusions

In summary, dispersive SnO_2 nanosheets with the thickness of 10 nm have been successfully synthesized through a simple hydrothermal method. The gas-sensing properties of our SnO_2 nanosheets-based sensor exhibits high response to ethanol, and fast response–recovery, good repeatability to CO. Typically, the response and recovery times of the sensor using SnO_2 nanosheet to 200 ppm CO are about 1 and 3 s. These results indicate that the present SnO_2 nanosheets are promising for gas sensors.

Acknowledgements

This work was supported by the National Nature Science Foundation of China (Nos. 60625301, 61006055, and 61074172).

References

[1] H.C. Hsu, W.W. Wu, H.F. Hsu, L.J. Chen, Growth of high-density titanium silicide nanowires in a single direction on a silicon surface, Nano Lett. 7 (2007) 885–889.
[2] Y.C. Chou, W.W. Wu, S.L. Cheng, B. Yoo, N. Myung, L.J. Chen, K.N. Tu, In-situ TEM observation of repeating events of nucleation in epitaxial growth of nano $CoSi_2$ in nanowires of Si, Nano Lett. 8 (2008) 2194–2199.
[3] Y.J. Li, M.Y. Lu, C.W. Wang, K.M. Li, L.J. Chen, Stable and highly sensitive gas sensors based on semiconducting oxide nanobelts, Appl. Phys. Lett. 88 (2006) 143102.

[4] J.H. He, C.L. Hsin, J. Liu, L.J. Chen, Z.L. Wang, Piezoelectric gated diode of a single ZnO nanowire, Adv. Mater. 19 (2007) 781–784.
[5] A. Kolmakov, Y. Zhang, G. Cheng, M. Moskovits, Detection of CO and O_2 using tin oxide nanowire sensors, Adv. Mater. 15 (2003) 997–999.
[6] V.V. Sysoev, B.K. Button, K. Wepsiec, S. Dmitriev, Toward the nanoscopic "Electronic Nose": hydrogen vs carbon monoxide discrimination with an array of individual metal oxide nano- and mesowire sensors, Nano Lett. 6 (2006) 1584–1588.
[7] F. Sun, W. Cai, Y. Li, L. Jia, F. Lu, Direct growth of mono- and multilayer nanostructured porous films on curved surfaces and their application as gas sensors, Adv. Mater. 17 (2005) 2872–2877.
[8] Y.L. Wang, X.C. Jiang, Y.N. Xia, A solution phase precursor route to polycrystalline SnO_2 nanowires that can be used for gas sensing under ambient conditions, J. Am. Chem. Soc. 125 (2003) 16176–16177.
[9] A. Kay, M. Grätzel, Dye-sensitized core-shell nanocrystals: improved efficiency of mesoporous tin oxide electrodes coated with a thin layer of an insulating oxide, Chem. Mater. 14 (2002) 2930.
[10] M.S. Arnold, P. Avouris, Z.W. Pan, Z.L. Wang, Field-effect transistors based on single semiconducting oxide nanobelts, J. Phys. Chem. B 107 (2003) 659–663.
[11] Y. Liu, J. Dong, M. Liu, Well-aligned "nano-box-beams" of SnO_2, Adv. Mater. 16 (2004) 353–356.
[12] Z.R. Dai, Z.W. Pan, Z.L. Wang, Growth and structure evolution of novel tin oxide diskettes, J. Am. Chem. Soc. 124 (2002) 8673–8680.
[13] Y. Lilach, J.P. Zhang, M. Moskovits, A. Kolmakov, Encoding morphology in oxide nanostructures during their growth, Nano Lett. 5 (2005) 2019–2022.
[14] D.F. Zhang, L.D. Sun, J.L. Yin, C.H. Yan, Low-temperature fabrication of highly crystalline SnO_2 nanorods, Adv. Mater. 15 (2003) 1022–1025.
[15] E. Comini, G. Faglia, G. Sberveglieri, Z.W. Pan, Z.L. Wang, Stable and highly sensitive gas sensors based on semiconducting oxide nanobelts, Appl. Phys. Lett. 81 (2002) 1869.
[16] J.J. Vijaya, L.J. Kennedy, G. Sekaran, M. Bayhan, M.A. William, Preparation and VOC gas sensing properties of Sr(II)-added copper aluminate spinel composites, Sens. Actuators B 134 (2008) 604–612.
[17] M.H. Xu, F.S. Cai, J. Yin, Z.H. Yuan, L.J. Bie, Facile synthesis of highly ethanol-sensitive SnO_2 nanosheets using homogeneous precipitation method, Sens. Actuators B 145 (2010) 875–878.
[18] J. Zhang, S.R. Wang, Y. Wang, M.J. Xu, H.J. Xia, Sh.M. Zhang, W.P. Huang, X.Z. Guo, S.H. Wu, Facile synthesis of highly ethanol-sensitive SnO_2 nanoparticles, Sens. Actuators B 139 (2009) 369–374.
[19] Y.J. Chen, L. Nie, X.Y. Xue, Y.G. Wang, T.H. Wang, Linear ethanol sensing of SnO_2 nanorods with extremely high sensitivity, Appl. Phys. Lett. 88 (2006) 083105.
[20] Q. Wan, Q.H. Li, Y.J. Chen, T.H. Wang, X.Y. He, J.P. Li, C.L. Lin, Fabrication and ethanol sensing characteristics of ZnO nanowire gas sensors, Appl. Phys. Lett. 84 (2004) 3654.
[21] Y.X. Liang, Y.J. Chen, T.H. Wang, Low-resistance gas sensors fabricated from multiwalled carbon nanotubes coated with a thin oxide layer, Appl. Phys. Lett. 85 (2004) 666.
[22] A.A. Firooza, A.R. Mahjouba, A.A. Khodadadib, Effects of flower-like, sheet-like and granular SnO_2 nanostructures prepared by solid-state reactions on CO sensing Mater, Chem. Phys. 115 (2009) 196–199.
[23] D.F. Zhang, L.D. Sun, G. Xu, C.H. Yan, Size-controllable one-dimensional SnO_2 nanocrystals: synthesis, growth mechanism, and gas sensing property, Phys. Chem. Chem. Phys. 8 (2006) 4874–4880.
[24] L.H. Qian, K. Wanga, Y. Li, H.T. Fang, Q.H. Lu, X.L. Ma, CO sensor based on Au-decorated SnO_2 nanobelt, Mater. Chem. Phys. 100 (2006) 82–84.
[25] C.S. Moon, H.R. Kim, G. Auchterlonie, J. Drennan, J.H. Lee, Highly sensitive and fast responding CO sensor using SnO_2 nanosheets, Sens. Actuators B 131 (2008) 556–564.
[26] G. Korotcenkov, B.K. Cho, Thin film SnO_2-based gas sensors: film thickness influence, Sens. Actuators B 142 (2009) 321–330.
[27] G. Korotcenkov, V. Brinzari, J.R. Stetter, I. Blinov, V. Blaja, The nature of processes controlling the kinetics of indium oxide-based thin film gas sensor response, Sens. Actuators B 128 (2008) 51–63.
[28] G. Korotcenkov, M. Ivanov, I. Blinov, J.R. Stetter, Kinetics of indium oxide-based thin film gas sensor response: the role of "redox" and adsorption/desorption processes in gas sensing effects, Thin Solid Films 515 (2007) 3987–3996.
[29] C.N. Xu, J. Tamaki, N. Miura, N. Yamazoe, Grain size effects on gas sensitivity of porous SnO_2-based elements, Sens. Actuators B 3 (1991) 147–155.

Biographies

Peng Sun received his MS degree from State Key Laboratory of Superhard Materials, Jilin University, China in 2009. He entered the PhD course in 2010, majored in microelectronics and solid state electronics. Now, he is engaged in the synthesis and characterization of the semiconducting functional materials and gas sensors.

Yang Cao received her BS degree from the Electronics Science and Engineering department, Jilin University, China in 2010. Presently, she is a graduate student, majored in microelectronics and solid state electronics.

Jun Liu received his BS degree from the Electronics Information and Engineering department, Jilin University, China in 2010. Now, he is a graduate student, majored in integrated circuit engineering.

Yanfeng Sun obtained his PhD from Jilin University of China in 2007. Presently, he is working as Lecturer in Electronics Science and Engineering department of Jilin University. His current research interests are nanoscience and gas sensors.

Jian Ma received his MS in 2009 from Jilin University of China at the Electronics Science and Engineering department. Presently, he is working as Technical Assistant in Electronics Science and Engineering department of Jilin University. His current research interests are gas sensor, the design and fabrication of micro-hot plates.

Geyu Lu received his BS and MS degree in electronic sciences from Jilin University, China in 1985 and 1988, respectively, and PhD degree in 1998 from Kyushu University in Japan. Now he is a professor of Jilin University, China. Presently, he is interested in the development of functional materials and chemical sensors.